CFD CALCULATION OF THE PRESSURE DROP THROUGH A RUPTURE DISK

L. Mengali, D. Melideo[1], F. Moretti[1], F. D'Auria[1], O. Mazzantini[2]

1 University of Pisa, 2 Nucleoeléctrica Argentina S.A.

ABSTRACT

The pressure drop through the Rupture Disk device (RD) of the boron injection system of the nuclear power plant of Atucha I is investigated and results are compared with experimental data taken from several tests performed at an experimental facility in Erlangen. Air and water tests are available for different flow rates with an overall Reynolds number ranging from 3000 to 17000. ANSYS CFX 11.0 with RANS SST turbulence modelling has been applied and several sensitivity analyses were performed addressing different geometries, boundary conditions, roughness values, turbulence models and other numerical settings, thus trying to comply with the recommendations of the Best Practice Guidelines. Attempts are made to assess the influence of modelling assumptions due to the lack of some information in the experimental data. Comparison between simulation and experiments shows quite a good agreement.

1 INTRODUCTION

The fast boron injection is a backup system for the fast shutdown of the Atucha I and II reactors, the main system being constituted by the control rods. The boron injection is meant to be actuated during certain postulated accidental scenarios, including the large break LOCA. The system consists of four injecting lines, each including one pressurized air tank, two fast acting valves, two boric acid solution tanks, one rupture disk and one injecting lance. The injection is powered by the pressurized air in the tank as soon as the intervention signal makes the valves open. One of the critical components of the system is the so-called rupture disk, which is a device containing a rupture membrane that, during normal operation, separates the high pressure ambient of the reactor pressure vessel from the low pressure one in the boron tanks. When the injection system intervenes, the pressurization of the injecting circuit causes the membrane to break, thus allowing the borated solution to rapidly flow into the moderator tank. Pressure losses across the rupture disk device influence the injection time and hence are important for the fast response of the system. For this reason several experimental tests were performed to study such a pressure drop.
In the following paragraphs a short description of the test facility is given. The computational grid and parameters for the CFD simulations are described and results are compared with experimental data.

2 EXPERIMENTAL SETUP

The experimental test document (Weber, 1971) describes tests performed before 1971 in the experimental facility of Erlangen for the assessment of the pressure drop through the RD. The test apparatus is sketched in Figure 1. It consists in a long series of pipes of different diameters, installed upstream and downstream the RD, where pressure is measured at stations shown in the figure. The test fluid (water or air) is driven through the system in order to measure the pressure drop between the two stations adjacent to the RD.

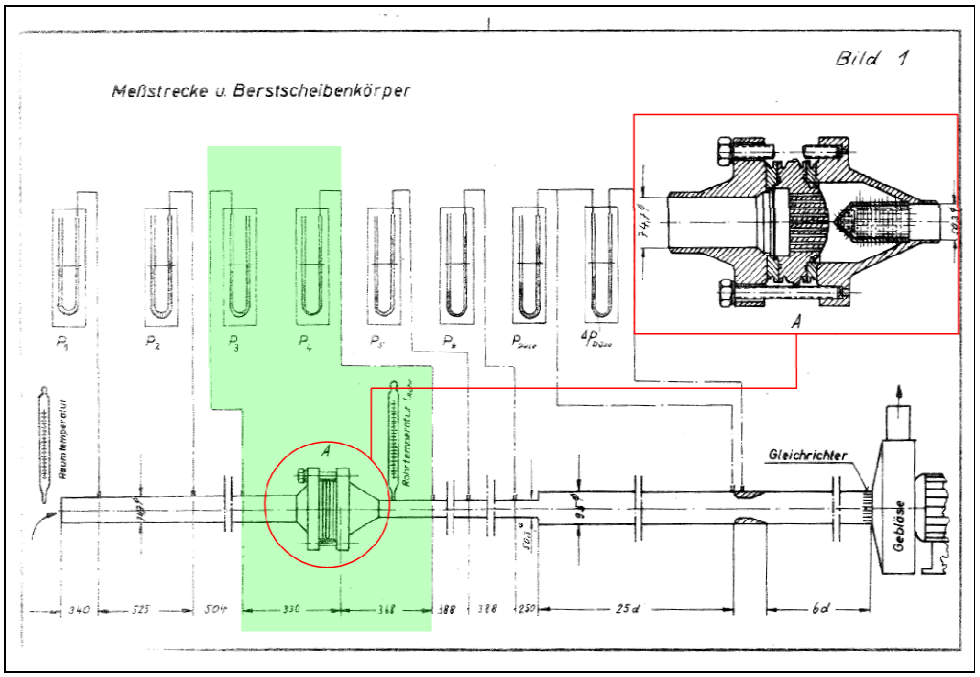

Figure 1: Experimental Apparatus

The RD (Figure 2) is mainly constituted by the following components:

- *Primary and secondary flanges*: connecting to the rest of the apparatus (piping)
- *Burst Insert*: provided with 171 holes (ϕ 4mm) in contact with the steel membrane
- *Steel membrane*: designed to break for a pressure difference across it of 31.5 bar
- *Strainer cylinder*: provided with 340 holes (ϕ 4mm), act as a filter for the debris of the broken membrane

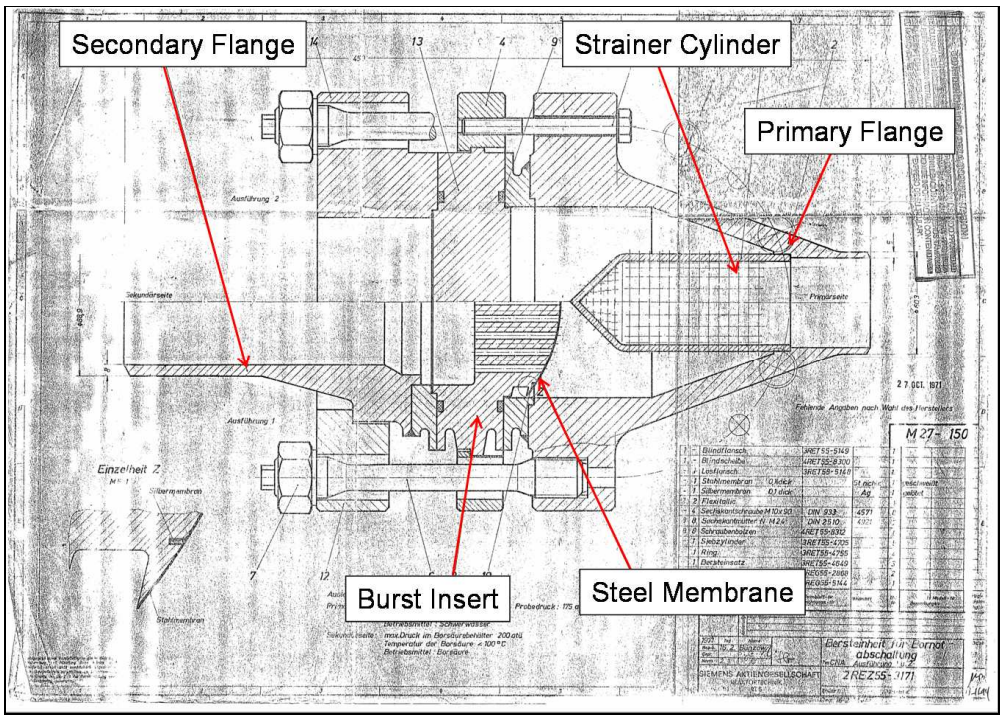

Figure 2: Assembly Drawing of the Rupture Disk Device

Several tests were performed in order to study the behaviour of the flow through the RD after the break of the steel membrane:

- single test with air and volumetric flow rate of 380 m^3/h
- series of tests with air studying the influence of the channels Reynolds number in the range $3000 \le \mathrm{Re}_{ch} \le 16000$
- series of tests with water studying the influence of the channels Reynolds number in the range $7000 \le \mathrm{Re}_{ch} \le 17000$
- series of tests with closed strainer holes studying the influence of holes occlusion.

Where Re_{ch} is the Reynolds number calculated at the holes in the burst insert.

The occlusion tests were performed in order to study the influence of covered holes in the case when debris of the steel membrane blocks the flow through some holes.
No tests were performed at the actual Reynolds number (heavy water volumetric flow rate of 212 m^3/h with $\mathrm{Re}_{ch} > 10^5$) since the apparatus was not designed for such a value.
Water tests show a higher pressure loss coefficient compared to air for the same Reynolds number. The document explains that entrapped air bubbles in the flow may be the reason for such behaviour. This hypothesis is supported by the fact that there is a narrowing in the difference while the water mass flow rate increases (with subsequent decrease in the relative air content). On the other hand no information is available about such air inclusions and therefore cannot be accounted for in the CFD calculations.

3 CFD MODEL

The aim of the CFD simulations is to reproduce the experimental tests in terms of pressure drops and pressure loss coefficients for the validation process. The experimental tests chosen for the comparison were:

- single air test with a volumetric flow rate of 380 m^3/h
- series of tests with air studying the influence of Reynolds number
- series of tests with water studying the influence of Reynolds number

Eight steady-state CFD calculations were set-up (four for air and four for water) imposing different inlet velocities, in order to compare the results for different Reynolds numbers.

3.1 Computational Grids

The computational domain includes the fluid volume inside the RD (coloured region in Figure 3). In particular the entire fluid domain was divided into several sub-domains:

- *Pre-Burst*: internal volume of the secondary side connecting flange
- *Burst Channels*: 171 longitudinal channels in the burst insert
- *Post-Burst*: volume included between the burst insert and the strainer cylinder
- *Strainer Holes*: 340 holes (14x20 radial and 60 frontal) in the strainer cylinder
- *Strainer*: internal volume of the strainer cylinder and of the primary side flange

Owing to the symmetry of the RD, the computational domain was chosen as a quarter of the entire fluid domain (a 90-degree sector), as shown in Figure 4.

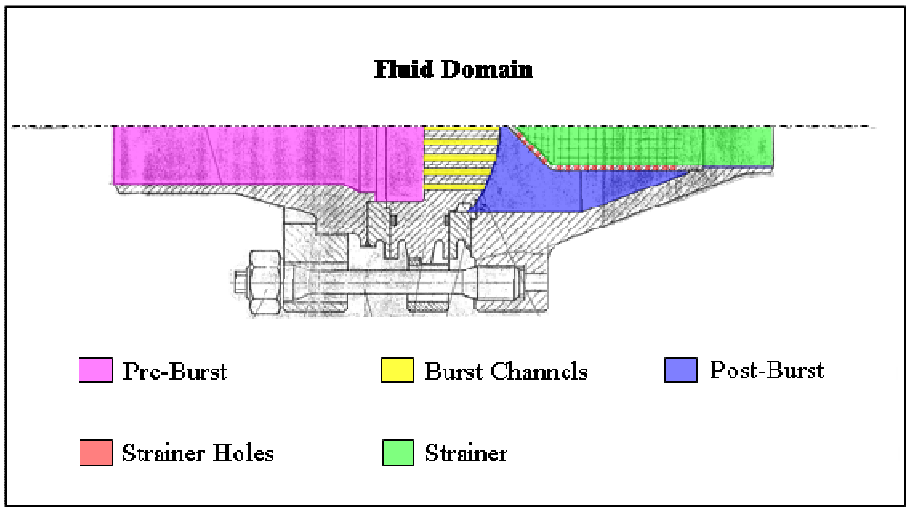

Figure 3: Fluid Domain and Domain Sub-Divisions

The domain has the following boundaries for application of boundary conditions (Figure 4):

- Inlet (in cyan)
- Outlet (in red, not visible in the figure)
- Two symmetry planes defining the 90°-sector (in grey)
- Walls: all other boundaries (in green)

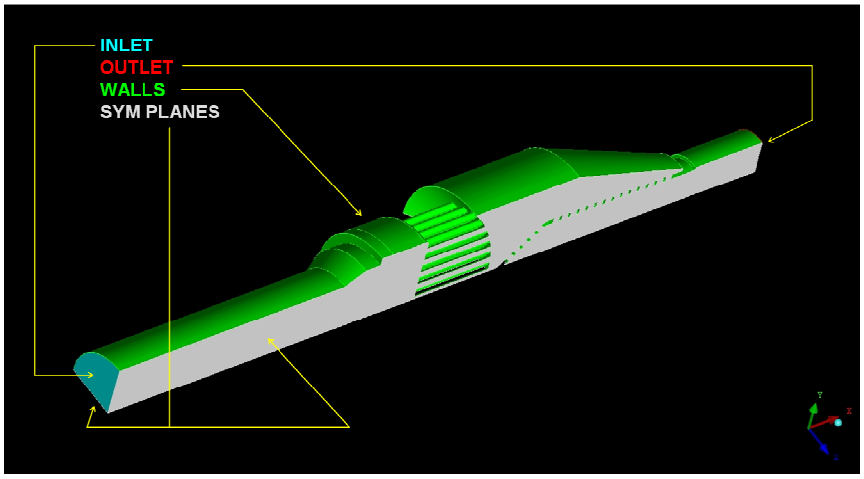

Figure 4: Computational Domain and Boundaries

The grid is generated using the Octree volumetric meshing algorithm available in ICEM CFD and is mainly tetrahedral with 3 prism layers near wall boundaries. A higher mesh density in the holes region (both burst insert and strainer) and wall mesh refinement are imposed.. The prism layer total height is 0.15 mm with first node distance of about 0.032 mm (refinement height ratio of 1.5). The total number of nodes

Table 1: Mesh Information

N° of nodes	Tetra	Prism	ICEM Quality	
~ 2 800 000	**~ 10 000 000**	**~ 1 900 000**	**> 0.3** (for more than 99% elements)	**< 0.2** (for less than 0.03% elements

Figure 5 shows some features of the developed grids. In particular different mesh densities near the wall and for the holes are visible at the symmetry plane (top) and the prism layer features are shown for transverse and longitudinal sections of the burst insert holes (bottom)

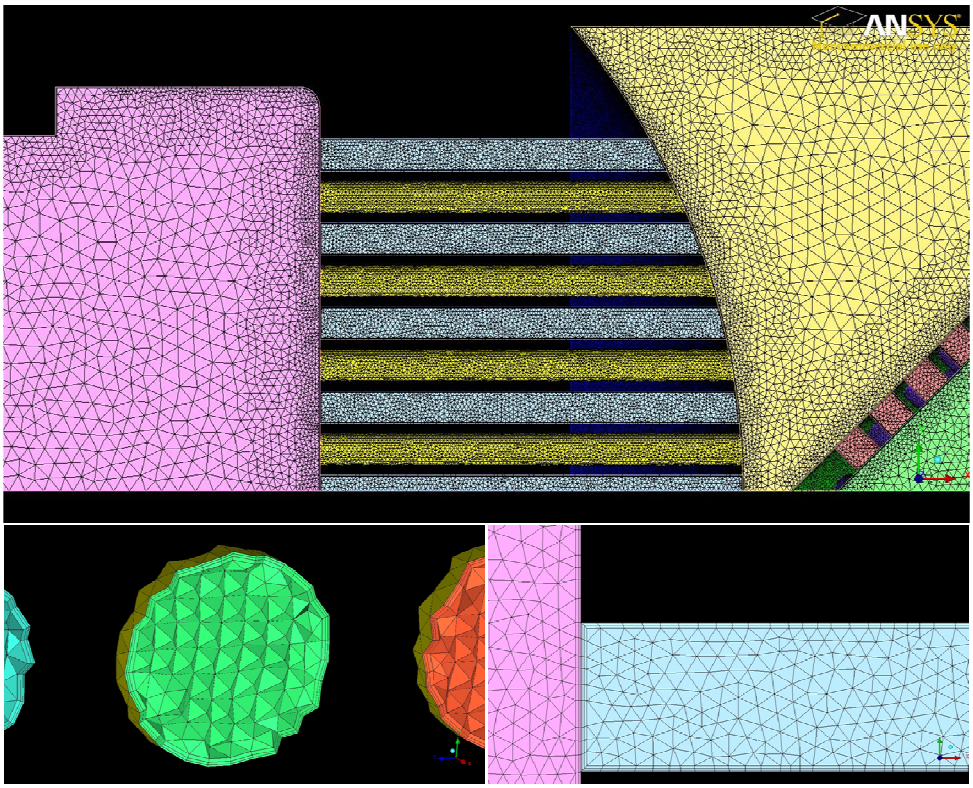

Figure 5: Mesh Features

3.2 Simulation Setup and Boundary Conditions

The simulations were performed using the computational grid mentioned above and the CFD package ANSYS CFX 11.0. In addition to the reference calculations, several sensitivity analyses were performed in order to provide relevant information on the influence of some boundary or geometric features and numerical settings.
The turbulence is accounted for with the Shear Stress Transport (SST) model. A convergence criterion based on the following two conditions is applied to all the calculations performed:

- the Root Mean Square (RMS) normalized values of the equation residuals must drop by at least 4 orders of magnitude, and the asymptotic region possibly be reached;
- the flow fields (velocity, pressure, temperature fields etc.) must be stabilized.

Although at least a second order advection scheme is suggested for good quality results (Mahaffy, 2007), a first order (upwind) numerical discretization scheme was chosen in order to enhance the poor convergence behaviour of the calculations. On the other hand such scheme intensifies diffusive phenomena, (through an additional “numerical” viscosity) with respect to higher order schemes, thus leading to higher pressure drops.

The following boundary conditions have been imposed to the computational domain:

- *Inlet*:
    - velocity (uniform profile)
    - turbulence intensity (5%, CFX default value)
    - eddy viscosity ratio (10, CFX default value)

- *Outlet*: "opening" pressure-controlled condition with "zero gradient" turbulence option, as recommended by CFX 11 user manual
- *Symmetry planes*: symmetry conditions
- *Walls*:
    - No-slip condition

A total of eight simulations are performed for the comparison with experimental results. All the Reynolds numbers are calculated with the mean bulk velocity and diameter at the burst channels, **Error! Reference source not found.** shows the main features of these calculations:

Table 2: Main Simulations Performed

Simulation ID's	Working Fluid	Inlet Velocity	Re (burst channels)
RDair_n171_UW_base	Air @ 25°C	25.2893 m/s	12 716
RDair_n171_UW_u10	Air @ 25°C	10 m/s	5 028
RDair_n171_UW_u20	Air @ 25°C	20 m/s	10 057
RDair_n171_UW_u50	Air @ 25°C	50 m/s	25 142
RDwater_n171_UW_u1	Water @ 25°C	1 m/s	8 704
RDwater_n171_UW_u2	Water @ 25°C	2 m/s	17 409
RDwater_n171_UW_u3	Water @ 25°C	3 m/s	26 114
RDwater_n171_UW_m60	Water @ 25°C	14.3749 m/s	125 130

For the first and last case, the inlet velocity is calculated from the respective volumetric flow rate value, while the other cases are chosen in order to obtain values of the Reynolds number in the range given in the test document. In particular, the volumetric flow rate for the single air test case is taken from the experimental document (380 m^3/h) and the value from the last water case is taken as the value in nominal working condition (0.06 m^3/s) which returns a mass flow rate of 59.82 kg/s.

3.3 Sensitivity Analyses

Based on the RDair_n171_UW_base simulation, taken as the reference case, the following sensitivity analyses are performed:

- sensitivity on geometry
    - 171 Burst Channels with different hole locations
- sensitivity on boundary conditions
    - wall roughness included (16 μm)
    - turbulence intensity: Low (1%)
    - turbulence intensity: High (10%)
- sensitivity on modelling
    - air as ideal gas
    - k-ε turbulence model
    - k-ω turbulence model
    - Six-equation Baseline Reynolds Stress Model (BSLRSM)
- sensitivity on numerical settings
    - Fixed Blend (0.2) advection scheme
    - HR (High Resolution) advection scheme for the last water case

Table 3 shows the sensitivity analyses performed:

Table 3: Sensitivity Analyses Performed

Sensitivity analysis	Simulation ID	Reference case ID
Geometry		
171 Burst Channels	RDair_n171bis_UW	RDair_n171_UW_base

Boundary Conditions		
Wall roughness (16 μm)	RDair_n171_rough	RDair_n171_UW_base
Turbulence Intensity 1%	RDair_n171_LowT	RDair_n171_UW_base
Turbulence Intensity 10%	RDair_n171_HighT	RDair_n171_UW_base
Modelling		
Air as ideal gas	RDair_n171_UW_idealgas	RDair_n171_UW_base
k-ε turbulence model	RDair_n171_UW_keps	RDair_n171_UW_base
k-ω turbulence model	RDair_n171_UW_komega	RDair_n171_UW_base
BSLRSM turbulence model	RDair_n171_UW_BSLRSM	RDair_n171_UW_base
Numerical Settings		
Fixed Blend (0.2)	RDair_n171_Blend20	RDair_n171_UW_base
High Resolution	RDair_n171_HR	RDair_n171_UW_base

4 CFD RESULTS

The target variable is the pressure loss coefficient of the RD calculated as the area averaged total pressure difference between inlet and outlet divided by the dynamic pressure at the outlet. The performed calculations did not converge adequately when the High Resolution (suggested by ANSYS) advection scheme is chosen. For this reason the first-order upwind advection scheme has been used for all calculations. All the eight studied cases show quite similar behaviours: RMS residuals drop between 4 and 5 orders of magnitude and max oscillations in the control variables are around 0.3% – 1% (relative value).
Although relatively poor, this convergence behaviour can be considered acceptable for the present study, as it is bringing calculation errors smaller than the experimental uncertainties. Since all the main calculations show qualitatively similar behaviour, the qualitative analysis of results is performed only for the RDair_n171_UW_base case, while the quantitative results comparison includes also the remaining seven reference calculations.

4.1 Wall Distance y^+

The maximum value of y+ is around 25 for both the air test (u = 50 m/s) and water test (u = 3 m/s) and located in the last holes of the strainer cylinder. The mean value over the whole walls is around 8. Maximum and mean values for the RDwater_n171_UW_m60 case are respectively 115 and 30. Figure 6 shows a detail of the Y+ contours for the RDair_n171_UW_u50 case.

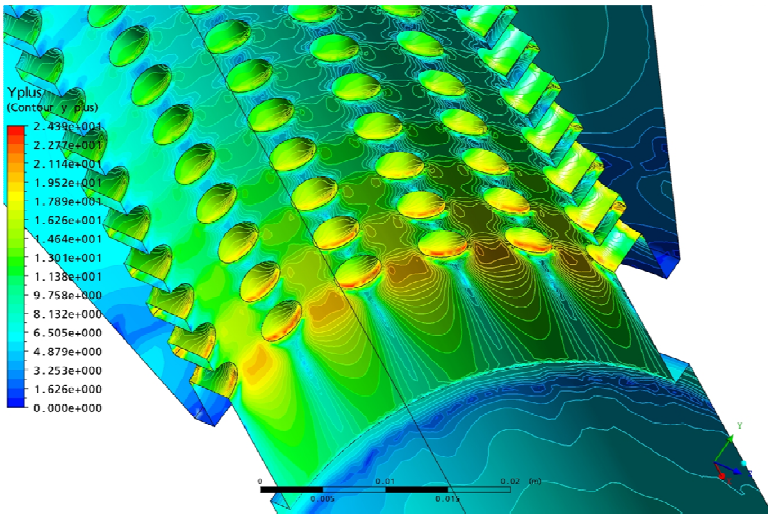

Figure 6: Y^+ contours for the RDair_n171_UW_u50

4.2 Velocity and Pressure Fields

Figure 7 shows the velocity vector field on a symmetry plane. The highest velocities, of about 100 m/s, occur in the last holes of the strainer cylinder (down-flow direction). In particular, most of the flow at the exit of the burst insert moves around the strainer cylinder towards the back of the primary flange and is strongly accelerated there by the high pressure drop to the strainer cylinder and finally to the outlet. A strong re-circulation region is formed just outside the burst insert, near the lateral wall of the primary flange.

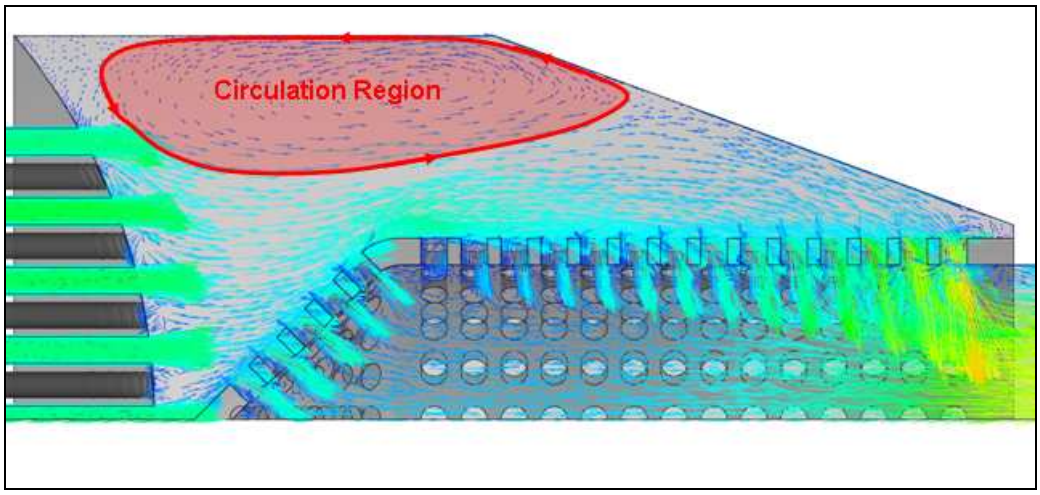

Figure 7: Velocity Vector Field on the Symmetry Plane

The total pressure field is shown in Figure 8 where the main losses are at the exit of the burst channels and in the back of the strainer cylinder after the last holes. All these regions are near re-circulations due to sudden expansions in the flow. It is interesting to note how the total pressure is not uniformly distributed at the outlet.

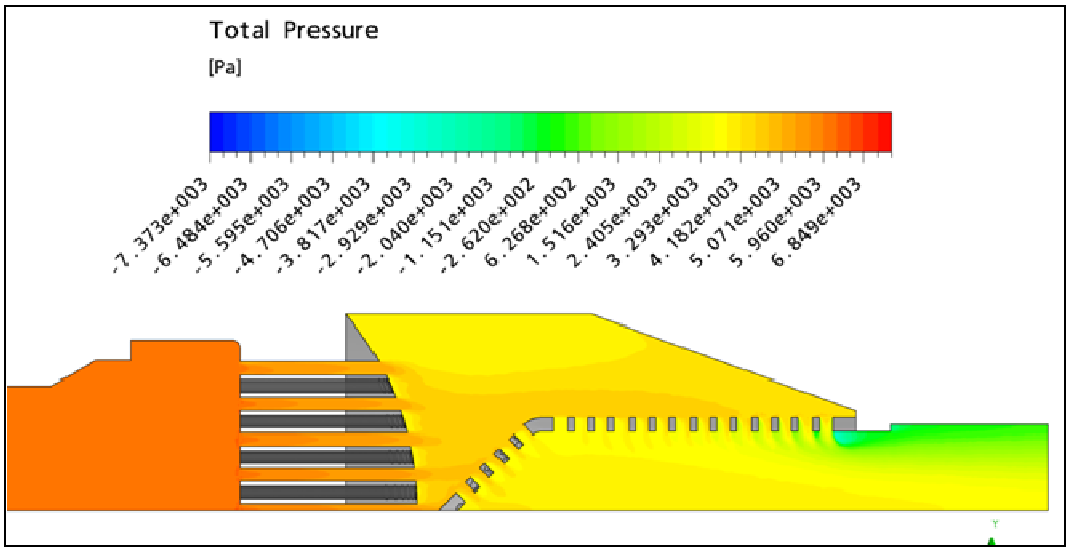

Figure 8: Total Pressure Field on the Symmetry Plane

Table 4 shows the pressure losses for all the cases studied:

Table 4: Pressure Losses

Case ID	Total Pressure Drop [kPa]	Loss Factor k_{tot}
Air		
RDair_n171_UW_base	4.40	2.63
RDair_n171_UW_u10	0.74	2.83
RDair_n171_UW_u20	2.78	2.66
RDair_n171_UW_u50	16.79	2.57
Water		
RDwater_n171_UW_u1	5.90	2.68
RDwater_n171_ UW_u2	22.86	2.60
RDwater_n171_ UW_u3	50.77	2.56
RDwater_n171_ UW_m60	1127.86	2.48

5 SENSITIVITY ANALYSES

Several sensitivity studies are performed in order to assess the influence of some uncertainties in geometric and flow parameters.
A different arrangement of the burst insert holes is studied since only the longitudinal cross section of the device is available in the experiment document and the geometry used in the simulations is deduced from a slightly different newer design. The new arrangement of the holes is shown in Figure 9, where 28 holes are moved from the inner part (in red) to the peripheral region (in blue).
Different settings for turbulence level and wall roughness are studied since no detailed information is available for inlet and wall conditions.
The influence of compressibility is investigated because the velocity can locally reach values greater than 100 m/s (Mach numbers greater than 0.3).
Finally sensitivity on turbulence model and advection scheme was analyzed.

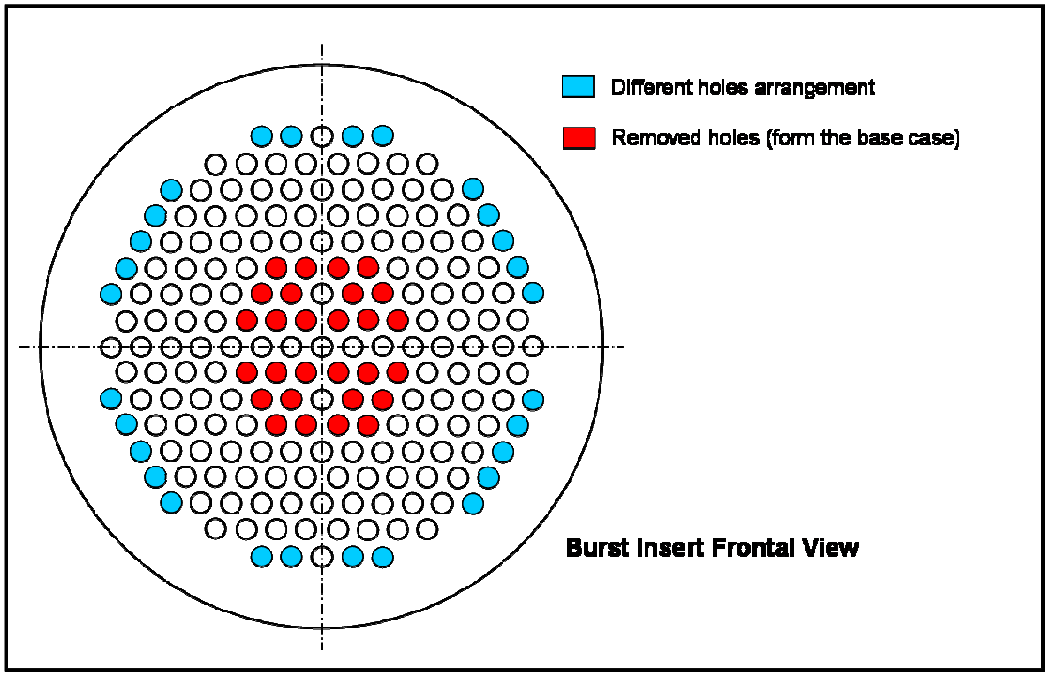

Figure 9: Different Burst Holes Arrangement

Table 5 shows the calculated loss factor for the sensitivity analyses:

Table 5: Sensitivity Analyses Results

Simulation ID	Total Loss Factor k_{tot}	Relative Error
Reference Case		
RDair_n171_UW_base	2.63	-
Sensitivity on Geometry		
RDair_n171bis_UW	2.58	-2.0%
Sensitivity on Boundary Conditions		
RDair_n171_rough	2.75	+4.5%
RDair_n171_LowT	2.62	-0.6%
RDair_n171_HighT	2.65	+0.8%
Sensitivity on Working Fluid		
RDair_n171_UW_idealgas	2.61	-0.6%
Sensitivity on Turbulence Model		
RDair_n171_UW_keps	2.66	+1.0%
RDair_n171_UW_komega	2.73	+3.9%
RDair_n171_UW_BSLRSM	2.64	+0.5%
Sensitivity on Numerical Settings		
RDair_n171_Blend20	2.58	-2.1%
RDair_n171_HR*	2.39	-9.1%

* very poor convergence (RMS residuals drop ~ 10^{-3})

The different arrangement of burst holes, while having quite a strong influence on the flow structure, has a moderate effect on the loss factor. For the compressibility, the effect is negligible, with local temperature differences (theoretically absent for incompressible flows) of a few degrees Celsius. The other results of the sensitivity analyses show relatively small differences from the reference case except for the rough case and the κ-ω turbulence model. Special attention should be given to the advection scheme: in particular, the High Resolution case returns a value of the loss factor well below the reference case, suggesting an overestimation of the calculated loss factor due to the numerical enhanced diffusive phenomena connected to the use of a first order advection scheme. However such result should be handled with care since the convergence behaviour for this case is poorer.

6 VALIDATION

For the single air test, the experiment report gives two numerical values: the overall loss factor ξ, calculated from the pressure loss between measurements stations placed at a distance of 698 mm and the concentrated loss factor ξ' obtained subtracting the friction losses extrapolated from the previous and following duct sections in order to evaluate the concentrated loss factor relative to the RD.
In order to compare the results obtained by the CFD analysis with experiments it is necessary to calculate the loss factor ξ*, both concentrated and from friction, relative to a length of the RD of 450 mm (the actual length of the developed geometry). Assuming that the friction loss factor varies linearly with length the value for the comparison can be calculated as:

$$\xi^* = \xi' + \frac{L_{MODEL}}{L_{3-4}}(\xi - \xi') = 2.44 + \frac{450}{698}(2.56 - 2.44) \approx 2.52 \quad (1)$$

Table 6 shows the comparison between the reference case RDair_n171_UW_base and the experimental result.

Table 6: Validation of the Single Air Test

Experimental Loss Factor ξ*	Calculated Loss Factor k_{tot}	Relative Error
2.52	2.63	+4.4%

For the Reynolds influence test, experiment results are given only in the form of graphs. Figure 10 shows the comparison for the validation study, experimental curves are obtained through graphical interpolation from the graphs in the experiment document.

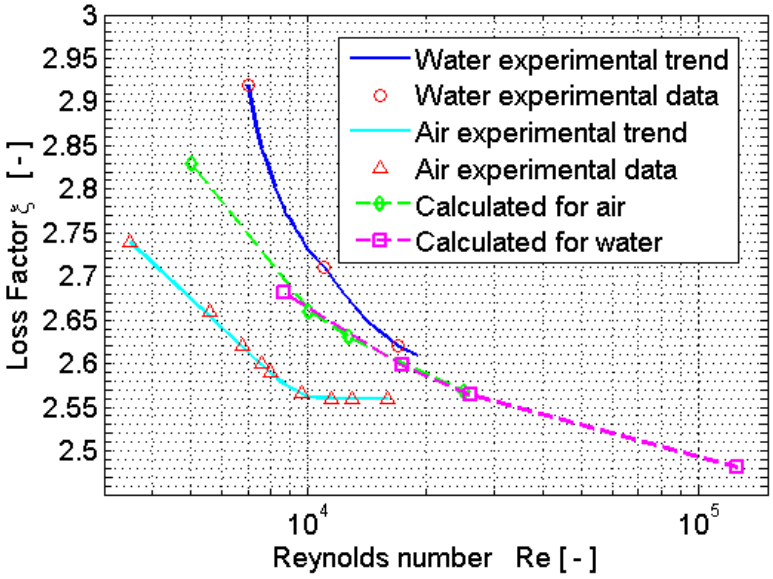

Figure 10: Validation of the Reynolds Influence

The relative error ranges from 2.0% to 5.8% for air tests and from 0.8% to 3.7% for water tests. While experimental tests for water and air are quite different for equal Reynolds numbers, the calculated values nearly overlap (as should be); this different behaviour is probably due to the air inclusion in the water tests mentioned above (Paragraph 2) as suggested by the author of the experimental test document. Another different trend can be found in the presence of an asymptotic behaviour for the air experimental case that is missing in calculated results. This difference is most probably connected to the wall roughness, which plays a more and more important role for growing Reynolds numbers, while it is not systematically considered in the calculations (it is accounted for in a sensitivity analysis only).

7 CONCLUSIONS

The performed CFD analyses focused on the validation of the pressure losses through the Rupture Disk Device of the fast boron injection in the nuclear power plant of ATUCHA I. Some information crucial to the development of the grid and to the set-up of the CFD calculations is missing or difficult to read from the experiment documentation available, hence several assumptions were made in order to completely define the problem. Eight base calculations with different working fluid and inlet velocities were set-up for validation purposes. Moreover, ten additional sensitivity analyses were performed to provide information about the influence of some of the uncertainties introduced by the assumptions made.

The convergence behaviour of the calculations is acceptable if the first order upwind scheme is used. This leads to some over prediction of the loss factor due to the numerical diffusivity introduced. However, the comparison with experimental data shows reasonable agreement with relative error below 5% for most of the cases.

The sensitivity on advection scheme shows a relatively strong influence on the results. Normally, the use of higher order schemes will decrease the calculated pressure drop leading to a better match with experimental results; however, in this case such choice is not advisable due to the poorer convergence behaviour.

REFERENCES

Weber, “Der Stromungswiderstand von Berstscheibenk orpern des Borsaure Noteinspeisesystems CNA”, (1971)

Mahaffy J. et al., “best practice guidelines for the use of CFD in nuclear reactor safety applications” NEA/CSNI/R(2007)5, April 2007

ANSYS ICEM-CFD 11.0 User Manual, 2007

ANSYS CFX-22.0 User Manual, 2007